ADVANCED FUNCTIONAL MATERIALS
www.afm-journal.de

Rapid and Continuous Hydrodynamically Controlled Fabrication of Biohybrid Microfibers

*Michael A. Daniele, Stella H. North, Jawad Naciri, Peter B. Howell, Stephen H. Foulger, Frances S. Ligler, and André A. Adams**

Cell encapsulation is critical for many biotechnology applications including environmental remediation, bioreactors, and regenerative medicine. Here, the development of biohybrid microfibers comprised of encapsulated bacteria in hydrogel matrices produced on-chip using microfluidics is reported. The fiber production process utilizes hydrodynamic shaping of a cell-laden core fluid by a miscible sheath fluid. Production of the fibers containing viable bacteria was continuous in contrast to the more typical methods in which cells infiltrated or were attached to prepared fibers. The biohybrid fibers were composed of poly (ethylene glycol dimethacrylate) matrices and individually both *E. coli* and *B. cereus* were explored as model cellular payloads. Post processing growth curves (24 h) of bacteria within fibers were in excellent agreement with that of controls suggesting minimal impact. Finally, the biohybrid fibers showed even distribution of encapsulated cells and >90% cell viability.

1. Introduction

Applications for immobilized bacteria include controlled delivery of biofertilizers or biopesticides,[1] bioreactors,[2] bioremediation,[3] environmental sensors,[4,5] and microbial fuel cells.[6] A popular method for bacterial attachment is the growth of biofilms on suspended particles or solid substrates.[7,8] However, biofilm-mediated immobilization does not protect the cells from mechanical or chemical damage; consequently, sustaining high levels of viable bacterial cells within these systems for extended periods is tenuous at best.[1,9] Synthetic materials that encapsulate cells offer more protection from damage during use than immobilizing the cells on a surface, but may block transport of nutrients or targeted chemicals to the cells. Hydrogels have been widely explored for encapsulation because of biocompatibility and facile control of pore size, for example, as bioactive constituents encapsulated in hydrogels include enzymes,[10] bacterial,[11,12] and mammalian cells.[13]

The combination of hydrogel chemistry and fiber morphology provides an ideal platform for the encapsulation of cells for many large-scale applications, e.g., biofertilizers and biopesticides.[1] While the surface area-to-volume ratio (SA:V) of the hydrogels is inherently high, organizing the hydrogels into fibers can be used to promote the spatial distribution of cells and flux of liquids containing essential nutrients or chemical targets to the cells. Depending on the application, the fibers can be used individually as tubes or in concert as woven mats for applications such as sensing, filtration, tissue engineering or wound healing.

Common polymer fiber production methods, including melt extrusion, casting, and electrospinning, often require cytotoxic chemicals, complex processing tools, or procedures incompatible with maintaining cell viability. The melt extrusion process produces unique fibers with intricate dies; however, highly-crosslinked, physically robust hydrogels are incompatible with melt processing. Casting fibers using fused silica capillaries as molds is limited by its poor reproducibility and small batch production.[14] Electrospinning has been adopted as a popular method to produce biohybrid fibers;[15] however, electrospinning is not suitable for the in situ encapsulation of viable cells. Electrospinning with postfabrication crosslinking has been reported to induce bacterial cell death of up to 50% of the cells, and has also been shown to be incompatible with maintaining any viability of mammalian cultures post encapsulation.[16,17] Recent alternatives for fabrication of polymer fibers utilize "in-flow" processing, e.g., hydrodynamic extrusion or microfluidic casting. Although hydrodynamic extrusion circumvents the cytotoxic parameters of melt extrusion, this process is still restricted by complex dies, and limited chemistries.[18] Microfluidic casting provides a facile route for producing complex shaped fibers, but this process utilizes cytotoxic organic solvents.[19]

We report a simple one-step strategy using a single microfluidic device that continuously produces hydrogel fibers of tunable cross-section containing viable cells. Conventional nozzle-in-channel devices create core-sheath flow to control

Dr. M. A. Daniele, Prof. S. H. Foulger
Center for Optical Materials Science and Technologies
School of Materials Science and Engineering
Clemson University
Clemson, SC 29634, USA
Dr. S. H. North, Dr. J. Naciri, Dr. P. B. Howell,
Dr. F. S. Ligler, Dr. A. A. Adams
Center for Bio/Molecular Science and Engineering
Naval Research Laboratory
4555 Overlook Ave, SW Washington, DC, 20375 USA
E-mail: andre.admas@nrl.navy.mil

DOI: 10.1002/adfm.201202258

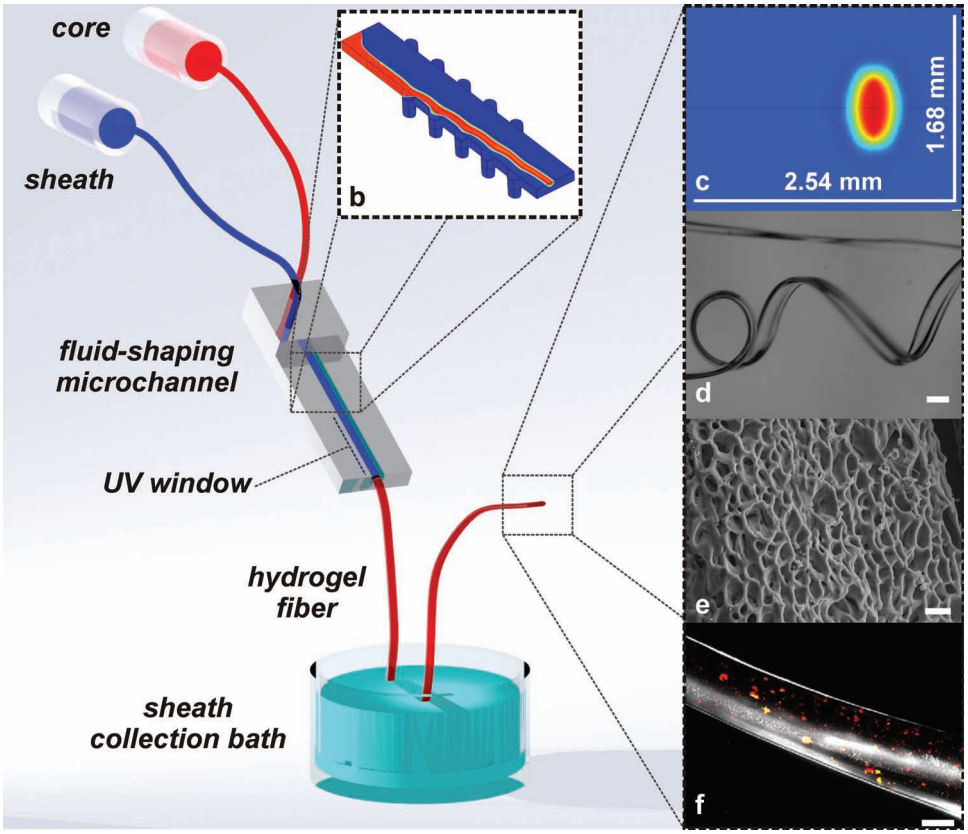

Figure 1. a–f). An illustration of the method for the fabrication of fibers. a) Sheath and core solutions are introduced in parallel to the channel. Recessed grooves hydrodynamically shape the sheath fluid (blue) around the core fluid (red). A detailed schematic of the microchannel is provided in Figure S2. b) Simulation of fluid shaping by recessed diagonal geometries. c) A vertical cross-section down the length of the channel showing the fluid shape after passing through the geometric-shaping zone. The core component (red) is surrounded by a diffusion layer (yellow/green) and the sheath fluid (blue). The dimensions of the microchannel were 2.54 mm × 1.68 mm. d) An optical micrograph of a microfiber, scale bar: 500 µm and e) SEM micrograph of the fiber surface showing the representative porosity of the PEGDMA hydrogel fibers, scale bar: 10 µm. f) Confocal micrograph compression of the fluorescence of viable bacteria within the fibers, scale bar: 200 µm.

fiber diameter,[20] the hydrogels and cells passing through the nozzle are subjected to cytotoxic shear forces. In comparison, shear stress is significantly reduced during fiber shaping by enveloping a laminar core within a sheath flow using grooves embedded into the channel walls to hydrodynamically focus the core within the sheath fluid. This approach enables the injection of viscous pre-polymer reagents infused with biological constituents with minimal clogging. Compared to microfluidic casting approaches, the rapid photoinitiated polymerization in the microfluidic channel avoids the cytotoxicity caused by organic solvents as well as osmotic pressure changes. In the continuous single-step process reported here, cells are localized in the hydrodynamically constrained core flow, and upon exposure to light, the pre-polymer core forms a crosslinked biohybrid fiber. In addition, the sheath stream can shape the fibers prior to polymerization; this provides the ability to fabricate larger flat fibers that may have increased strength and higher SA:V than round fibers with the same cross-sectional area. The laminar flow and photopolymerization conditions maintain the viability of the cells during the fiber fabrication process.

2. Results and Discussion

Figure 1 illustrates the production method for biohybrid microfibers that utilize hydrodynamic focusing and rapid UV polymerization. A pre-polymer solution including the cells was introduced into the microchannel adjacent to the sheath fluid (Figure 1a). Five diagonal grooves recessed into the top and bottom surfaces of the microchannel at 45° angles directed the sheath fluid across the channel; thereby, enveloping and shifting the core fluid toward the center of the microchannel, as indicated in Figure 1b. To design a version of this device capable of producing fibers with desired size and shape, microchannel flow simulations were carried out with the COMSOL Multiphysics modeling tool. Taking advantage of the device's symmetry, only half of the microchannel was modeled (Figure 1b). Figure 1c shows a simulation of the vertical cross-section down the length of the 5-groove channel. The simulation indicated the formation of an elliptical core flow. By varying the number and geometry of the shaping grooves, different fiber morphologies can be produced.[19] A detailed description of the design, fabrication and operation of the microchannel device,

simulation procedure and additional models are provided in the Supporting Information (Figure S1 and Figure S2). Photoinitiated polymerization of the core fluid was achieved by irradiating the fluid in situ with a UV curing lamp (λ_{peak} = 365 nm, 100 mW/cm^2) as it traversed the microchannel. The residence time of the fluid within the microchannel was dependent on flow rate and ranged from 1.50–1.59 s. The production of fibers was continuous with consistent shape, and the sheath fluid was easily removed using an aqueous collection bath.

The pre-gel solution utilized as the core fluid was composed of poly(ethylene glycol dimethacrylate) M_n = 750 g/mol (PEGDMA), and the biocompatible, water-soluble photoinitiator Irgacure 2959.[21,22] PEGDMA was chosen as the initial hydrogel due its rapid polymerization kinetics and the breadth of literature on its synthesis.[23–25] PEGDMA is appropriate for the systematic exploration of cell response to specific alterations in the methods for fabricating the hydrogel scaffold. In addition, pure PEGDMA hydrogels function as blank slates in biological systems; they are resistant to nonspecific adsorption of plasma proteins, and minimal cell interactions between the hydrogel and the mesh occur unless reactive functional groups are incorporated.[26,27] In this case, cell immobilization is strictly based on physical encapsulation within the hydrogel matrix. The sheath was an aqueous solution of poly(ethylene glycol) M_n = 400 g/mol, selected to approximately match the viscosity and hydrophilicity of the pre-gel solutions.

Fibers were produced from pre-gel solutions of 75, 50, and 25% (w/w) PEGDMA. Recent hydrogel spinning techniques required postfabrication stretching to control fiber size and shape, which imparts undue stress on the hydrogel network and bio-constituents;[28] in contrast, hydrodynamic focusing utilizes simple variations in the ratio of the sheath-to-core flow rates to control the dimensions of the fiber. Optical and scanning electron microscopies were employed to characterize the size and morphology of the hydrogel fibers (**Figure 2**). By decreasing the flow rate of the core fluid and holding the sheath flow rate constant, the long axis of the ribbon-like fibers was decreased from ≈500 to ≈100 μm. The size of the fibers was broadly controlled by the flow-rate ratios and polymer content (Figure S1,S3). The flow-rate ratios set general constraints on final fiber dimensions; however, polymer content determines mesh size and swelling, which results in the definitive dry and wet fiber dimensions. An illustrative, interconnected network of pores was observed on the surface of the fibers (Figure 2d–f). Evaporative drying of hydrogels causes internal pore collapse; therefore, to accurately quantify the mesh size, laser scanning confocal microscopy was used to visualize the internal mesh in the water-swollen state (Supporting Information, Table S3 and Video S3). Reducing the concentration of PEGDMA increased the observed mesh size from 3.0 ± 1.9 μm to 31.4 ± 6.3 μm. The dependence of mesh size on the ratio of PEGDMA:water is indicative of phase separation during polymerization.[29,30] Consequently, both the flow rates of the fluids and the concentrations of the pre-gel solution can be used to tune the final morphology and porosity of the fibers.

For the fibers to be effectively used for applications, they must be physically and thermally robust, confine the cells, and permit both transport of nutrients/targets and the egress of waste.[26,31] The thermal and hydration properties of the PEGDMA hydrogel fibers were determined using thermogravimetric analysis (TGA) and differential scanning calorimetry (DSC). After fabrication, fibers were immersed in water overnight to swell with water and remove unreacted pre-polymer. For TGA, the initial weight loss of samples corresponds to the evaporation of water from the fibers. For pre-gel concentrations of 75, 50, and 25% (w/w) PEGDMA and sheath:core flow rates of 800:50 μL/min (flow-rate ratio = 16:1), the water contents were 38, 50, and 77%, respectively (Figure S4, Supporting Information).

The thermal degradation temperature of fibers indicates their stability in the common temperature range for biological use. After the evolution of water (>100 °C), TGA showed no weight loss until temperatures between 375 and 400 °C were reached. This matched the expected temperature range for decomposition of a crosslinked network of poly(ethylene glycol).[29,32] Accordingly, differential thermograms showed proportionally increasing decomposition rates for higher concentrations of PEGDMA. DSC confirmed the uniformity of gelation of the fibers. Dried fibers exhibited a single glass-transition temperature (T_g) dependent on the concentration of PEGDMA in the pre-gel solution. The corresponding T_g were –37.9, –40.4, and –41.9 °C for 75, 50, and 25% (w/w) PEGDMA, respectively. By increasing the concentration of PEGDMA in the pre-gel solution, the T_g was increased. The data corroborated previous reports that water acts as a plasticizer/extender in the hydrogel network: during polymerization, water increases the free volume between polymer chains and causes increased chain mobility.[30]

The concentration of PEGDMA in the pre-gel solution and corresponding morphology of the derived fibers will also affect EWC (**Figure 3**). To analyze EWC, fibers were lyophilized for 24 h, transferred to a buffer solution, and incubated at 25 °C for periods of up to 2 h. Aqueous solutions of 0.1 M phosphate and 0.15 M saline were adjusted to pH 4, 7, and 10. The fiber samples were blotted with wet filter paper to remove excess water and weighed. EWC was calculated from Equation 1 where m_0 is the mass of the dry fiber and m_t is the mass of the hydrated fiber.

$$EWC = \frac{m_t - m_o}{m_o} \quad (1)$$

Fibers produced from a pre-gel solution containing 25% (w/w) PEGDMA reached EWC of 400% in less than 10 min. Fibers produced from a pre-gel solution containing 50% (w/w) and 75% (w/w) PEGDMA achieved EWC's of 120% and 60%, respectively, in as little as 5 min. The pH of the hydrating solution caused no significant effect on EWC. Poly(ethylene glycol) is a neutral polymer at low molecular weights; therefore, pH should not affect its hydration properties.[33] The rate of hydration is critical for providing a uniform and equilibrium state for the encapsulated cells. Either exceedingly rapid or slow hydration of the fibers would ultimately prove detrimental to the encapsulated cells.

Before encapsulation of cells in the hydrogel fibers, we examined the effects of long-wave UV irradiation and photoinitiator on cell viability (Figure S6, Supporting Information). Gram-positive *B. cereus* and Gram-negative *E. coli* bacteria were chosen as models for biohybrid fiber fabrication. They are

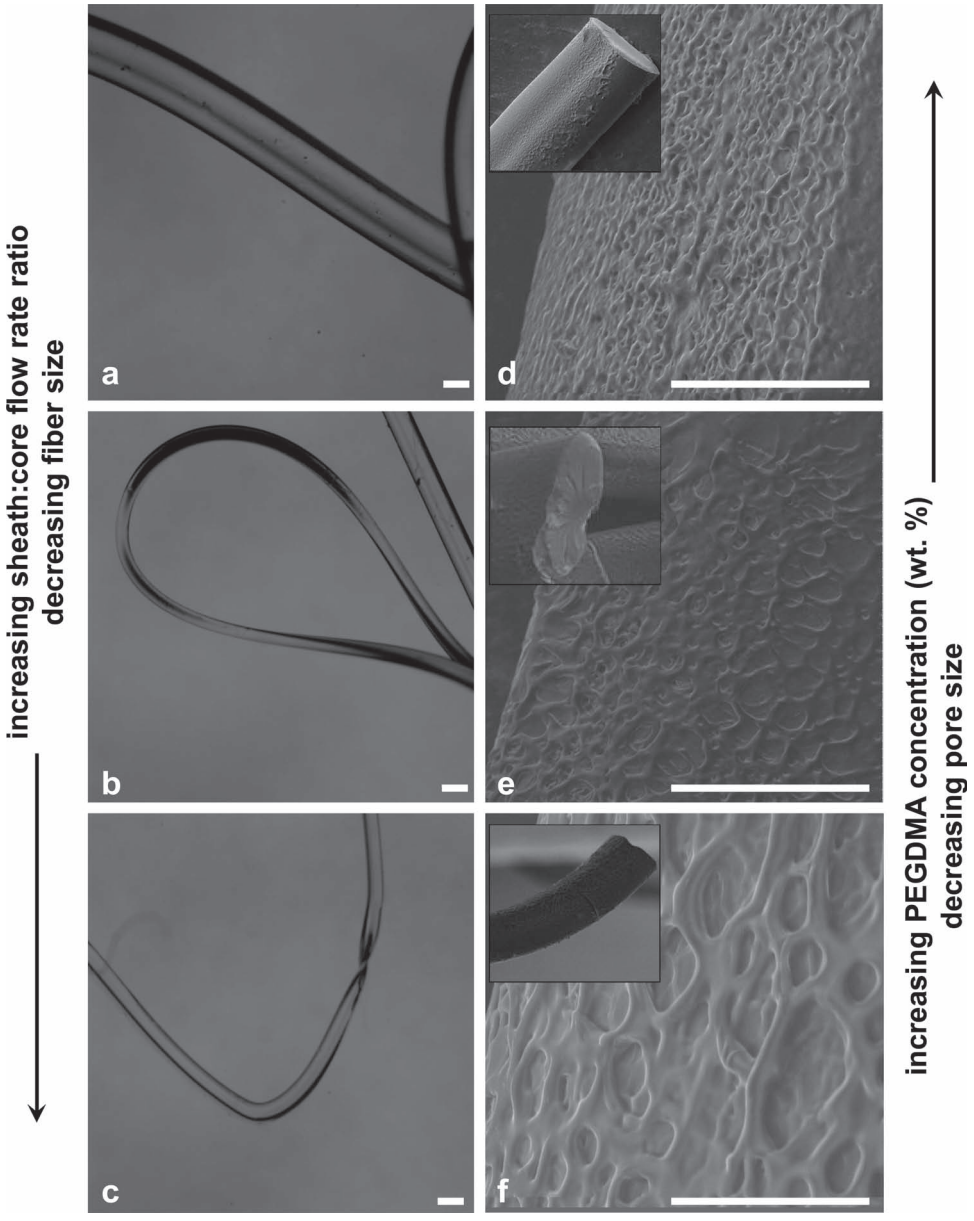

Figure 2. a–c) During the fabrication process, the dimensions of the fiber are also controlled by varying the sheath:core flow-rate ratios (16:1, 32:1, 80:1). Increasing the sheath:core flow rate ratio decreases the cross-sectional area. Fibers shown were produced from a pre-gel solution of 75% (w/w) PEGDMA. Micrographs of dried fibers were taken at 2× magnification. Hydrogel porosity was controlled by varying the concentration of PEGDMA in the pre-gel solution. d–f) Increasing concentrations of PEGDMA decreases mesh size. The mean Feret diameters and standard deviation (n = 6) for 75, 50, and 25% (w/w) PEGDMA fibers were 3.0 ± 1.9, 16.7 ± 2.8, and 31.4 ± 6.3 μm, respectively. Inset images are representative fibers at sheath:core flow rate of 800:25 μL/min. Scale bars: 100 μm.

well-characterized organisms and have been reported as viable candidates for genetically engineered whole-cell sensors, a potential application for these biohybrid fibers.[4,34,35] We evaluated the effects of the photoinitiator (Irgacure 2959) and the UV radiation (λ_{peak} = 365 nm, 100 mW/cm^2, 10 s) on the viability and subsequent growth rate. In multi-well plate growth experiments, *B. cereus* and *E. coli* cells were irradiated with UV in the presence and absence of the photoinitiator, and optical density (OD) readings were taken periodically over 15 hours at 600 nm. The growth curve in the absence of any treatment served as a reference. Timed comparisons of *B. cereus* cell growth as determined by OD_{600} measurements after treatment demonstrated that the photoinitiator and UV exposure have no significant effect on *B. cereus* viability and growth profile. In contrast, consistent with a previous report by Hollaeder et al.,[36] UV-treated *E. coli* grew at a decelerated rate and to a 17% lower cell density than untreated or photoinitiator-treated *E. coli*. The prolongation of the "lag-phase" of *E. coli*, and the decreased cell density indicate a slight impact on the growth of *E. coli* after UV irradiation.

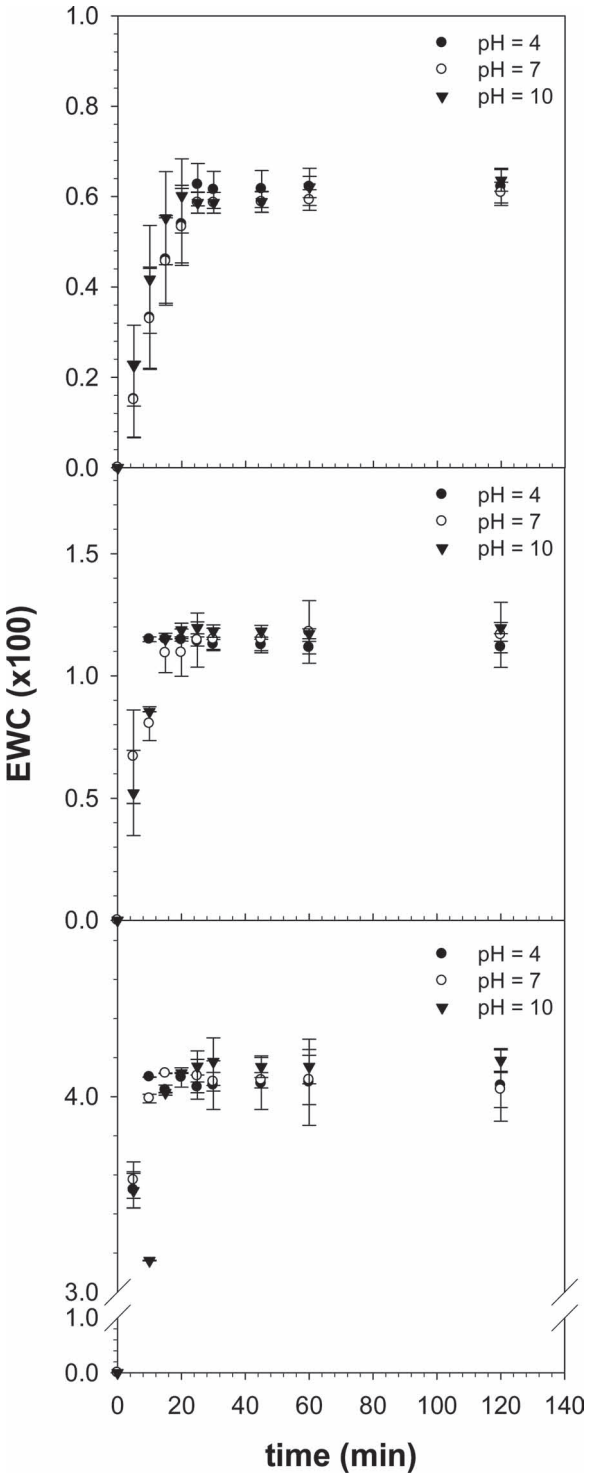

Figure 3. a–c) Fibers produced from different concentrations of PEGDMA were equilibrated at pH = 4, 7, and 10. The fibers were produced from solutions of (a) 75%, (b) 50%, and (c) 25% (w/w) PEGDMA at sheath:core flow rates of 800:50 μL/min. Data points are the mean and error bars are the standard deviations of the samples (n = 3).

To evaluate bacterial encapsulation efficiency of the hydrogel photopolymerization process, *B. cereus* cells were pre-stained with Invitrogen LIVE/DEAD *BacLight* fluorescent dyes (L-7012) (**Figure 4**a) and suspended directly in a PEGDMA pre-polymer solution (6×10^6 cells/mL). For all biohybrid fibers, the core fluid contained PEGDMA diluted with PBS (pH = 7.4). The fluid was injected at 800:50 μL/min sheath:core flow rates. The labeled bacteria were imaged post-fiber production on an inverted confocal microscope. Fluorescence micrographs of the fibers showed that bacterial cells were uniformly dispersed throughout the length and breadth of the hydrogel microfibers (Figure 4b,c).

As it is critical that the encapsulation process does not compromise cell viability, metabolic activity and growth assays were performed with different bacterial cell populations to determine not only the biocompatibility of the hydrogel scaffold but also the impact of both the chemistry and processing on cell viability and proliferation. *B. cereus* and *E. coli* bacteria were each encapsulated into hydrogel microfibers, and the number of viable cells within the 3D scaffold was visualized with the vital stain 5-cyano-2,3-ditolyl tetrazolium chloride (CTC). In contrast to LIVE/DEAD stains that indicate the status of membrane integrity as opposed to "true" viability, CTC dyes react with electrons produced from redox reactions of actively respiring bacteria to form a red fluorescent formazan product signaling a working metabolism.[37] A green fluorescent probe (SYTO24) was used as a counterstain to identify all cells. Figure 4d–i shows representative images of the bacteria in the pre-gel solution and post-fiber production. *E. coli* and *B. cereus*, in solution and in fibers, show active cellular respiration as indicated by the red fluorescent formazan precipitation. A small population (<10%) of the cells of either species exhibited the green fluorescence of SYTO24 (Figure 4e,f,h,i), indicating that both Gram-positive and Gram-negative cells survive the fiber production processing and retain metabolic activity. Micrographs showed >90% viable cells, which is highly significant in contrast to electrospinning, which generates <50% cell survival rate.[14,15]

To further demonstrate the suitability of the hydrodynamically shaped fibers as hosts for the bacterial cells, a recombinant *E. coli* strain harboring pRSET-B/mCherry was encapsulated into the hydrogel fibers, and confocal images were taken immediately after fiber production and after four hours of incubation in growth media. The expression of fluorescent protein ($\lambda_{ex}/\lambda_{em}$ = 587/610) was used to monitor cell growth within fibers. The number of bacteria increased more than three times the initial density within the fiber after four hours of incubation in growth media, indicating that the fibers were sufficiently porous for efficient nutrient diffusion and waste exchange. To determine if the bacteria were inhibited from movement through the fibrous scaffold, fibers containing the cells were plated and cultured on standard agar plates. We observed significant bacterial colony formation about the fibers (Figure S7c,d, Supporting Information). Furthermore, the spreading of a mass of cells (Figure S7a, Supporting Information) to a more uniform distribution through the fiber (Figure S7b, Supporting Information) suggests bacterial migration within the hydrogel scaffolding. Taken together, these results demonstrate that the morphology and hydration properties of these PEGDMA fibers not only support efficient nutrient exchange to promote cell growth and proliferation, but also allow cell mobility within the microfibers.

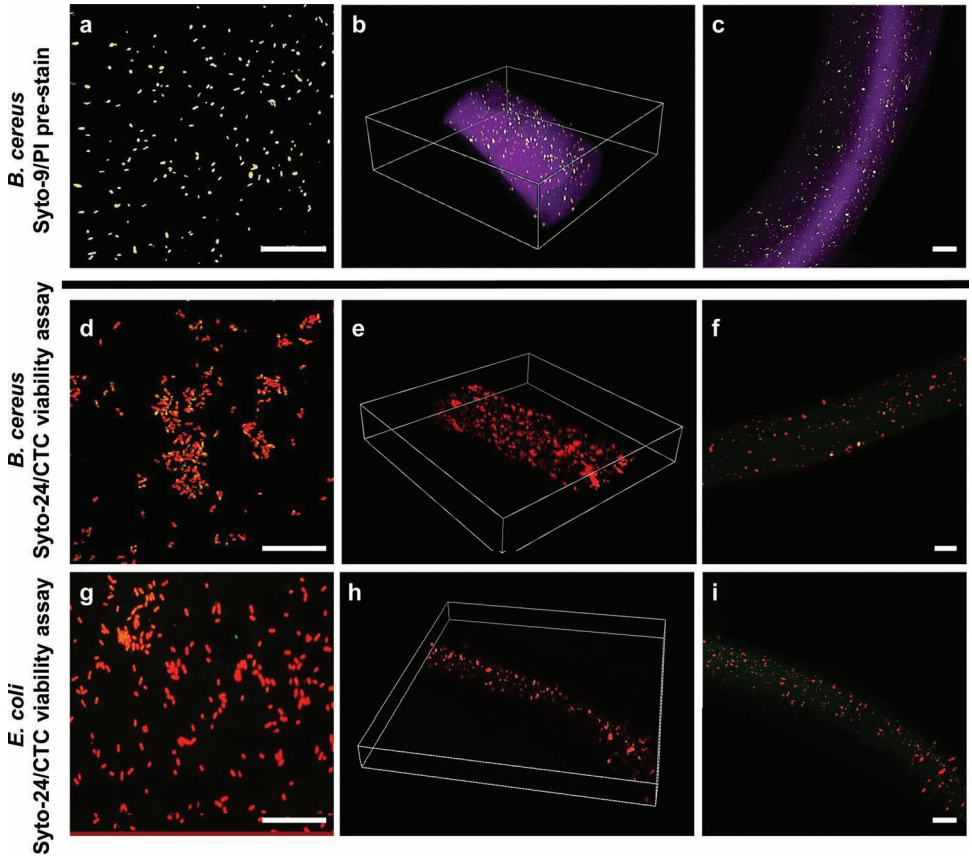

Figure 4. Confocal micrographs of prestained bacteria in the pre-gel solutions (a,d,g) and encapsulated in fiber (b,c,e,f,h,i). a–c) *Bacillus cereus* (*B. cereus*) were prestained with green fluorescent SYTO 9 (all bacteria) and propidium iodide (PI; nonviable cells only) to evaluate encapsulation efficiency and distribution of cells in the fiber. d–f) *B. cereus* and g–i) *Escherichia coli* (*E. coli*) treated with CTC to determine metabolic activity, as indicated by red fluorescent formazan product. SYTO 24 was used as counterstain. b,e,h) Images are z-stack confocal images of the entire thickness of the fibers. Hydrated fibers were stabilized and kept wet between two cover slips. c,f,i) Images are z-stack compressions of approximately half the fiber thickness to illustrate the density and uniformity of encapsulated cells. Scale bar: (a,d,g) 50 µm; (c,f,i) 100 µm.

3. Conclusions

In summary, we have presented a method based on microfluidics and hydrodynamic focusing for the continuous production of biohybrid fibers. By adjusting pre-polymer solutions and flow rates within the microchannel, we were able to tune the morphology, hydration, and thermal properties of the fibers. The methodology produced hydrogel fibers that sustained viable cells as demonstrated by the encapsulation and subsequent proliferation of *B. cereus* and *E. coli*. The described method differs from other hydrodynamic methods by removing the problematic "needle-in-channel" or "concentric annuli" form factors. Using integrated, shaping features and laminar flow reduces common fabrication problems like clogging or axial diffusion. Moreover, the hydrodynamic focusing within the microfluidic channel can provide a continuous process for in situ gelation. The flexibility in fiber size, shape and composition, coupled with benign photopolymerization conditions, surpasses other reported biohybrid fiber fabrication methods in terms of ease of the fabrication and resultant cell viability.

4. Experimental Section

Materials: PEGDMA and Irgacure 2959 (2-Hydroxy-4-(2-hydroxyethoxy)-2-methyl-propiophenone) were purchased from Sigma Aldrich (St. Louis, MO). Prior to mixing pre-gel solutions, the hydroquinone inhibitor was removed from the PEGDMA using an inhibitor removal column (column SDHR-4 from Scientific Polymer Products, Inc., Ontario, NY). Deionized water was obtained from a Millipore Sapphire System and exhibited a resistivity of 18.2×10^{18} ohm^{-1} cm^{-1}.

Microfluidic Fiber Production: The microchannel was direct-milled into a cyclic-olefin-copolymer (COC) to the dimensions, 2.54 mm × 1.68 mm (width × height). The dimensions of the 5 diagonal grooves were 0.64 mm × 0.84 mm (width x depth) and were spaced 3 mm apart.

The pre-gel solution was prepared in PBS by mixing PEGDMA (75, 50, 25% (w/w)) and I2959 (0.1% (w/w)). For the encapsulation of cells, a suspension of cells in PBS (6×10^6 cells/mL) was incorporated into the core solution. The sheath solution was prepared by mixing PEG M_n = 400 Da and water (50% (v/v)). Sheath and core fluids were injected into the microchannel via syringe pumps.

Thermal Analysis: Thermogravimetric analysis was performed at a heating rate of 10 °C/min in a nitrogen atmosphere up to 600 °C with a Thermal Analysis 2900 TGA instrument. The mass of the samples varied from 5 to 9 mg. The water/polymer content was determined at the onset of the first derivative of weight loss with respect to temperature reaching

zero. Thermal degradation temperature values reported were taken at the peak maximum of the first derivative of weight loss with respect to temperature. Differential scanning calorimetry was performed from –65 to 20 °C at a rate of 5 °C/min with a Thermal Analysis 2920 DSC equipped with R40 refrigerant cooling accessory. The carrier gas was nitrogen at a flow rate of 50 mL/min. All DSC samples were hermetically sealed and cycled thrice, with reported values taken from the third cycle. Reported T_g values were taken at the peak maximum in the curve of the first derivative of heat flow.

Biohybrid Fiber Production and Characterization: *E. coli* XL-1 Blue (Agilent Technologies, Santa Clara, CA) was cultured in Luria-Bertani broth (Difco BD Microbiology Systems, Sparks, MD) containing 12 μg/mL tetracycline at 37 °C. *E. coli* XL-1 Blue/pRSET-B mCherry was cultured in LB broth containing 100 μg/mL ampicillin at 37 °C. *B. cereus* (ATCC, Manassas, VA) was cultured in Tryptic Soy Broth (Difco BD) at 30 °C. For growth profiles, cells overnight cultures were inoculated in multiwell plates at a final $OD_{600} \approx 0.10$. Individual wells were treated with photoinitiator, irradiated with UV, or both. Growth profiles were obtained over a 15 h period. For encapsulation studies, overnight cultures were washed three times in phosphate buffered saline (PBS) and suspended in PBS prior to fiber production. Final concentrations of cells in the pre-gel solution were $\approx 10^6$ cells/mL.

Cellular activity of bacteria was determined by the BacLight RedoxSensor CTC vitality assay (Molecular Probes, Eugene, OR) following the manufacturer's instruction. This fluorometric assay is based on the ability of cells to convert 5-cyano-2,3-ditolyl tetrazolium chloride (CTC) into an insoluble, red fluorescent formazan product, and is an indicator of the level of respiratory activity of bacterial populations. Green fluorescent SYTO 24 was used as a counterstain. Fibers containing cells were incubated in the solution for 30 min and visualized under a confocal microscope.

Supporting Information

Supporting Information is available from the Wiley Online Library or from the author.

Acknowledgements

The authors thank Igor L. Medintz for providing the *E. coli* pRSET-B mCherry used herein. This work was supported by the Naval Research Laboratory (NRL) and the Office of Naval Research (ONR) 6.1 work unit MA041-06-4286. The views expressed here represent those of the authors and do not reflect those of NRL, the Navy, or the Department of Defense.

Received: August 9, 2012
Published online: September 11, 2012

[1] R. P. John, R. D. Tyagi, S. K. Brar, R. Y. Surampalli, D. Prevost, *Crit. Rev. Biotechnol.* **2011**, *31*, 211.
[2] M. A. Heitkamp, W. P. Stewart, *Appl. Environ. Microbiol.* **1996**, *62*, 4659.
[3] M. A. Heitkamp, V. Camel, T. J. Reuter, W. J. Adams, *Appl. Environ. Microbiol.* **1990**, *56*, 2967.
[4] A. Date, P. Pasini, A. Sangal, S. Daunert, *Anal. Chem.* **2010**, *82*, 6098.
[5] M. D. Pease, L. ShriverLake, F. S. Ligler, *Biosens. Chem. Sens. Technol.* **1995**, *613*, 33.
[6] O. Bretschger, J. B. Osterstock, W. E. Pinchak, S. Ishii, K. E. Nelson, *Microb. Ecol.* **2010**, *59*, 415.
[7] M. B. Cassidy, H. Lee, J. T. Trevors, *J. Ind. Microbiol.* **1996**, *16*, 79.
[8] K. Vijayaraghavan, Y. S. Yun, *Biotechnol. Adv.* **2008**, *26*, 266.
[9] H. Ben-Yoav, S. Melamed, A. Freeman, Y. Shacham-Diamand, S. Belkin, *Crit. Rev. Biotechnol.* **2011**, *31*, 337.
[10] C. Z. Wu, S. Bai, M. B. Ansorge-Schumacher, D. Y. Wang, *Adv. Mater.* **2011**, *23*, 5694.
[11] K. W. Wang, K. G. Lee, T. J. Park, Y. C. Lee, J. W. Yang, D. H. Kim, S. J. Lee, J. Y. Park, *Biotechnol. Bioeng.* **2012**, *109*, 289.
[12] S. Klein, J. Kuhn, R. Avrahami, S. Tarre, M. Beliavski, M. Green, E. Zussman, *Biomacromolecules* **2009**, *10*, 1751.
[13] D. Zaytseva-Zotova, V. Balysheva, A. Tsoy, M. Drozdova, T. Akopova, L. Vladimirov, I. Chevalot, A. Marc, J. L. Goergen, E. Markvicheva, *Adv. Eng. Mater.* **2011**, *13*, B493.
[14] Y. J. Heo, H. Shibata, T. Okitsu, T. Kawanishi, S. Takeuchi, *Proc. Natl. Acad. Sci. USA* **2011**, *108*, 13399.
[15] E. Zussman, *Polym. Adv. Technol.* **2011**, *22*, 366.
[16] M. F. Canbolat, C. Tang, S. H. Bernacki, B. Pourdeyhimi, S. Khan, *Macromol. Biosci.* **2011**, *11*, 1346.
[17] Y. Liu, M. H. Rafailovich, R. Malal, D. Cohn, D. Chidambaram, *Proc. Natl. Acad. Sci. USA* **2009**, *106*, 14201.
[18] M. Hu, R. S. Deng, K. M. Schumacher, M. Kurisawa, H. Y. Ye, K. Purnamawati, J. Y. Ying, *Biomaterials* **2010**, *31*, 863.
[19] A. L. Thangawng, P. B. Howell, J. J. Richards, J. S. Erickson, F. S. Ligler, *Lab Chip* **2009**, *9*, 3126.
[20] S. Shin, J.-Y. Park, J.-Y. Lee, H. Park, Y.-D. Park, K.-B. Lee, C.-M. Whang, S.-H. Lee, *Langmuir* **2007**, *23*, 9104.
[21] S. J. Bryant, C. R. Nuttelman, K. S. Anseth, *J. Biomater. Sci., Polym. Ed.* **2000**, *11*, 439.
[22] K. T. Nguyen, J. L. West, *Biomaterials* **2002**, *23*, 4307.
[23] J. L. Drury, D. J. Mooney, *Biomaterials* **2003**, *24*, 4337.
[24] J. Elisseeff, W. McIntosh, K. Anseth, S. Riley, P. Ragan, R. Langer, *J. Biomed. Mater. Res.* **2000**, *51*, 164.
[25] N. Garagorri, S. Fermanian, R. Thibault, W. M. Ambrose, O. D. Schein, S. Chakravarti, J. Elisseeff, *Acta Biomater.* **2008**, *4*, 1139.
[26] S. J. Bryant, K. S. Anseth, *J. Biomed. Mater. Res.* **2002**, *59*, 63.
[27] W. G. Koh, A. Revzin, M. V. Pishko, *Langmuir* **2002**, *18*, 2459.
[28] L. Leng, A. McAllister, B. Zhang, M. Radisic, A. Gunther, *Adv. Mater.* **2012**, *24*, 3650.
[29] J. A. Killion, L. M. Geeuer, D. M. Deuine, J. E. Kennedy, C. L. Higginbotham, *J. Mech. Behav. Biomed. Mater.* **2011**, *4*, 1219.
[30] Y. H. Wu, H. B. Park, T. Kai, B. D. Freeman, D. S. Kalika, *J. Membrane Sci.* **2010**, *347*, 197.
[31] J. A. DiRamio, W. S. Kisaalita, G. F. Majetich, J. M. Shimkus, *Biotechnol. Prog.* **2005**, *21*, 1281.
[32] H. Q. Lin, E. Van Wagner, J. S. Swinnea, B. D. Freeman, S. J. Pas, A. J. Hill, S. Kalakkunnath, D. S. Kalika, *J. Membrane Sci.* **2006**, *276*, 145.
[33] N. C. Padmavathi, P. R. Chatterji, *Macromolecules* **1996**, *29*, 1976.
[34] A. Date, P. Pasini, S. Daunert, *Anal. Chem.* **2007**, *79*, 9391.
[35] K. Yagi, *Appl. Microbiol. Biotechnol.* **2007**, *73*, 1251.
[36] A. Hollaender, *J. Bacteriol.* **1943**, *46*, 531.
[37] R. Zimmermann, R. Iturriaga, J. Beckerbirck, *Appl. Environ. Microbiol.* **1978**, *36*, 926.